The ISME Journal (2010) 4, 509–519

www.nature.com/ismej

ORIGINAL ARTICLE

Microtoming coupled to microarray analysis to evaluate the spatial metabolic status of *Geobacter sulfurreducens* biofilms

Ashley E Franks, Kelly P Nevin, Richard H Glaven[1] and Derek R Lovley
Department of Microbiology, University of Massachusetts, Amherst, MA, USA

Further insight into the metabolic status of cells within anode biofilms is essential for understanding the functioning of microbial fuel cells and developing strategies to optimize their power output. Cells throughout anode biofilms of *Geobacter sulfurreducens* reduced the metabolic stains: 5-cyano-2,3-ditolyl tetrazolium chloride and Redox Green, suggesting metabolic activity throughout the biofilm. To compare the metabolic status of cells growing close to the anode versus cells in the outer portion of the anode biofilm, anode biofilms were encased in resin and sectioned into inner (0–20 μm from anode surface) and outer (30–60 μm) fractions. Transcriptional analysis revealed that, at a twofold threshold, 146 genes had significant ($P<0.05$) differences in transcript abundance between the inner and outer biofilm sections. Only 1 gene, *GSU0093*, a hypothetical ATP-binding cassette transporter, had significantly higher transcript abundances in the outer biofilm. Genes with lower transcript abundance in the outer biofilm included genes for ribosomal proteins and NADH dehydrogenase, suggesting lower metabolic rates. However, differences in transcript abundance were relatively low (<threefold) and the expression of genes for the tricarboxylic acid cycle enzymes was not significantly lower. Lower expression of genes involved in stress responses in the outer biofilm may reflect the development of low pH near the surface of the anode. The results of this study suggest that cells throughout the biofilm are metabolically active and can potentially contribute to current production. The microtoming/microarray strategy described here may be useful for evaluating gene expression with depth in a diversity of microbial biofilms.
The ISME Journal (2010) **4,** 509–519; doi:10.1038/ismej.2009.137; published online 24 December 2009
Subject Category: integrated genomics and post-genomics approaches in microbial ecology
Keywords: *Geobacter*; microtoming; microbial fuel cell; transcription; biofilm

Introduction

One of the most surprising claims in the study of microbial respiration in past five years is the suggestion that microorganisms are capable of long-range electron transfer through the biofilms that form on the anodes of microbial fuel cells. The first evidence for this was the finding that the current output of microbial fuel cells of *Geobacter sulfurreducens* increased in direct proportion to the accumulation of biomass on the anode surface and with the increasing height of the anode biofilm (Reguera *et al.*, 2006). This suggested that cells at a substantial distance from the anode surface (that is, 50–100 μm) contributed to current production. The mechanisms for this potential long-range electron transfer have been intensively investigated and are still a matter of considerable debate (Lovley, 2006, 2008; Rittmann *et al.*, 2008; Logan, 2009).

A key assumption in this model for current production is that the cells at a distance from the anode are metabolically active. Indirect evidence for this in *G. sulfurreducens* anode biofilms (Reguera *et al.*, 2006) was the finding that cells throughout the anode biofilm fluoresced green when treated with the LIVE/DEAD BacLight bacterial viability kit from Molecular Probes (Eugene, OR, USA), designed to stain metabolically active cells green and metabolically inactive cells red (Boulos *et al.*, 1999).

Studies that have attempted to model the distribution of microbial activity in anode biofilms have suggested that different layers of the biofilm may have substantially different activities, but which layers are predicted to be most active depends on the assumptions incorporated into the modeling. For example, inital models predicted large variation in biofilm thickness and activity depending on the conductivity of the biofilm. In low conductive biofilms, it was estimated that almost all the active biomass would be located within the first 10 μm from the anode surface, with inert biomass dominating the biofilm at a distance greater then

Correspondence: AE Franks, Department of Microbiology, University of Massachusetts, Morrill IVN, 639 North Pleasant Street, Amherst, MA, USA.
E-mail: aefranks@microbio.umass.edu
[1]Current address: Center for Biomolecular Science and Engineering, Naval Research Laboratories, Washington DC, USA.
Received 24 August 2009; revised 5 November 2009; accepted 5 November 2009; published online 24 December 2009

3 μm (Marcus *et al.*, 2007). If a higher degree of conductance was assumed then thicker (ca. 50 μm) biofilms were predicted, but it was predicted that dual limitations of substrate concentration and localized potential differences within the biofilms would create a zone of 20–30 μm from the anode surface in which metabolic activity was the highest (Marcus *et al.*, 2007). When the release of protons within the biofilm was considered, it was predicted that the generation of low pH near the anode surface would limit metabolism in this zone, and that members of the biofilm at a distance from the anode would have higher rates of metabolism and contribute more to current production (Torres *et al.*, 2008).

Experimental evidence also suggests that the environment within anode biofilms is likely to be far from homogenous. For example, protons accumulate within anode biofilms of *G. sulfurreducens*, particularly near the anode surface, lowering the pH to levels that may inhibit metabolism (Franks *et al.*, 2009), as previously predicted in modeling studies (Torres *et al.*, 2008). Gradients in electron donor availability (Logan and Regan, 2006; Marcus *et al.*, 2007) and possibly other important environmental parameters are also likely. The impacts of these gradients on the metabolic status of cells throughout the anode biofilm are yet unknown.

Previous studies have demonstrated that it is possible to obtain significant insights into the functioning of anode biofilms through an analysis of gene transcript abundance. Genome-scale analysis of transcript abundance in cells growing in anode biofilms compared with transcript levels either in planktonic cells (Holmes *et al.*, 2005) or biofilm cells using fumarate as the electron acceptor (Nevin *et al.*, 2009), has revealed genes whose expression is specifically upregulated in cells producing current and has helped identify components, such outer-surface *c*-type cytochromes and pili, that seem to be important in electron transfer to the anode. Quantifying the level of transcripts of the gene for citrate synthase, a key gene in the tricarboxylic acid (TCA) cycle, demonstrated that citrate synthase transcript abundance within the anode biofilm was directly related to rates of current production (Holmes *et al.*, 2005). However, these previous studies evaluated transcript abundance within the complete anode biofilm, averaging any differences with depth in the biofilm, and could not account for potential differences in gene expression within different zones of the anode biofilm. This is a well-recognized limitation of transcriptional profiling in biofilms in general (An and Parsek, 2007).

The purpose of this study was to evaluate the hypothesis that there are major differences in the metabolic states between cells close to the anode surface and those at a greater distance from the anode. The new technique for evaluating gene expression at different depths in the anode biofilm, which was developed to address this question, is likely to have application for the study of gene expression in other types of biofilms as well.

Materials and methods

Staining for metabolic activity

Microbial reduction of metabolic stains in current-producing anode biofilms was imaged in the previously described microbial fuel cells that permit real-time imaging of the current producing biofilm (Franks *et al.*, 2009). These microbial fuel cells contain a solid graphite (grade G10; Graphite Engineering and Sales, Greenville, MI, USA) anode (0.81 cm^2) in a flow-through chamber (0.5 mm deep and 6.35 mm wide), which allows microscopic observation through a cover slip. The system was inoculated with *G. sulfurreducens* pRG5Mc that constitutively produces the fluorescent protein, mcherry, allowing fluorescent detection of the cells throughout the biofilm (Franks *et al.*, 2009). As previously described (Franks *et al.*, 2009), acetate (10 mM) was the electron donor for current production and fresh medium was continuously supplied at a flow rate of 0.1 ml min^{-1}.

Metabolic activity in the anode biofilms was evaluated using two different dyes. When in the oxidized state, 5-cyano-2,3-ditolyl tetrazolium chloride (CTC; BacLight RedoxSensor CTC Vitality Kit; Molecular Probes, Eugene, OR, USA) is soluble, colorless, and exhibits no fluorescence. Components of microbial electron transfer chains can reduce CTC to form a fluorescent intracellular, insoluble formazan (Rodriguez *et al.*, 1992). The CTC staining has been found to be useful in evaluating the metabolic state of a diversity of microorganisms, including *Geobacter* species, (Bhupathiraju *et al.*, 1999; Gruden *et al.*, 2003) and for localizing metabolic activity within biofilms (Schaule *et al.*, 1993; Huang *et al.*, 1995; Zheng and Stewart, 2004).

Redox Sensor Green reagent (Redox green; BacLight RedoxSensor Green Vitality Kit; Molecular Probes) yields green fluorescence when modified by bacterial reductases (Gray *et al.*, 2005). This dye has been used to detect metabolism of methylotrophs in lake sediments and may be less likely to inhibit microbial metabolism than CTC (Kalyuzhnaya *et al.*, 2008).

Fuel cells were grown to maximum power for staining. Medium was amended with CTC (5 mM) or Redox green (0.1 mM) and 10 ml of these solutions where injected into the anode chamber. The microbial fuel cells were incubated without flow in the dark for 30 min and then washed with fresh water acetate medium under a flow rate of 0.1 ml/min^{-1} for 30 min in the dark. The MFCs were immediately imaged with a Leica TCS SP5 microscope (Leica Microsystems GmbH, Wetzlar, Germany) with a HCX APO $\times 63$ (numerical aperture: 0.9) objective. Images where processed and analyzed with Leica LAS AF software (Leica). Consecutive line scanning

was used to detect CTC (excitation 488 nm/emission 630 nm), redox green (488 nm/emission 520) and mcherry red fluorescent protein that the cells constitutively produced (excitation 588/emission 600).

Transcriptional profiling

Studies on gene expression in *G. sulfurreducens* anode biofilms were conducted with wild-type *G. sulfurreducens* strain PCA (ATCC 51573, DSMZ 12127; Caccavo *et al.*, 1994). Cells were grown in 'H-cells' with a continuous flow of medium that contained acetate (10 mM) as the electron donor, as previously described (Reguera *et al.*, 2006), with the exception that the anode was modified to permit sub-sampling for microtoming. The usual 'stick' graphite anode, consisting of a $2.5 \times 7.5 \times 1.25$ cm piece of unpolished graphite, was replaced with two polished graphite electrodes of $2.5 \times 7.5 \times 0.1$ cm with grooves cut from the base to form five graphite 'fingers' of 0.2×0.1 cm. These dual electrodes provided a surface area of 60 cm^2, which is comparable to the 67.5 cm^2 of the usual electrodes and the fingers could be easily cut from the main body of the electrode for microtoming studies.

Electrodes with mature anode biofilms which had reached maximum power production levels (ca. 16 mA), corresponding to maximum biofilm thickness, were removed and 2 ml of RNAprotect Bacteria Reagent (Qiagen, Alameda, CA, USA) was immediately added to the side of the anode to be analyzed for gene expression. After 5 min, the graphite finger portions of the anode were cut into 5-mm sections without disturbing the anode biofilm. The RNAprotect Bacterial Reagent was removed by touching the other side of the electrode with a clean sterile Kim Wipe tissue. The sections were then covered in the low viscous hydrophilic London Resin White for 2 h at 4 °C. Excess London Resin White was then removed with a Kim Wipe tissue as before. Disposable Flat Embedding molds (#70906, Electron Microscope Services, Columbia, MD, USA) were placed on ice and prepared by wiping the inside with a sterile cotton wool bud with a single drop of accelerator (#02648-AB, SPI Supplies, West Chester, PA, USA). Excess accelerator was removed before the graphite anode sections were place into the mold. A volume of 10 ml of London Resin White resin was mixed with one drop of accelerator and immediately used to fill the space in the mold. Samples were allowed to cure overnight at 4 °C. This procedure produced a solid block of the intact biofilm associated with the graphite anode for sectioning (Figure 1).

The blocks were cut into 100-nm shavings with a 45° diamond cyro knife (Diatome, Hatfield, PA, USA) in a Leica Ultracut UCT ultramicrotome (Leica Microsystems, Bannockburn, IL, USA). Embedded sections were trimmed and three-dimensionally positioned to take 100-nm shavings parallel to the anode surface at a cutting speed of 1 mm s^{-1}. Inspection of the sample and knife position using a $\times 20$ magnification microscope of the ultramicrotome helped to ensure correct positioning. Shavings were pooled every 50 slices, representing 5-μm sections, and stored on ice. The block and knife were cleaned with a sterile brush and compressed air after each of these 50 slices allocates to reduce cross contamination of sections. The microtoming continued until the graphite surface was reached, as evidenced by black graphite visually apparent in the shavings. Sections were separated into inner (0–20 μm from the surface) and outer (30–60 μm from the surface) sections, flash frozen in an ethanol dry ice bath and stored at −80 °C until processed for RNA extraction.

The RNA was extracted from the biofilm sections with an acetone extraction method, as previously described (Holmes *et al.*, 2004). Samples were crushed with the end of sterile glass hockey sticks in 2-ml tubes and suspended in 800 μl of 4 °C TPE buffer (100 mM Tris–HCl, 100 mM KH_2PO_4, 10 mM EDTA (pH 8)). Plant RNA Isolation Aid (100 μl; Ambion, Austin, TX, USA) and 1 ml of −20 °C acetone was added. The mixture was mixed by

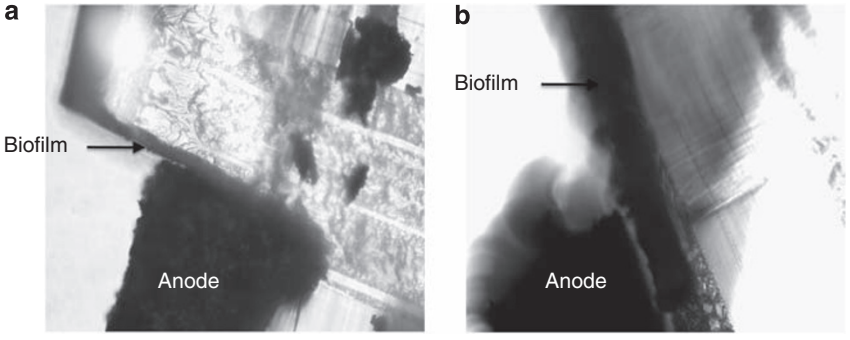

Figure 1 Current producing biofilm embedded in LR (London Resin) White resin. For these images under light (**a**) or phase-contrast (**b**) microscopy the resin was cut perpendicular to the biofilm surface in contrast to the microtoming in parallel used for sectioning, to reveal the full biofilm and its association with the graphite. The embedded biofilm is indicated by the arrows. Remains of the graphite anode, some of which was lost during the perpendicular cutting, is labeled as anode.

inverting ca. 40 times and then centrifuged at $16\,000 \times g$ for 10 min. The supernatant was discarded and 2 μl of Superase-In RNase inhibitor (Ambion) was added to the pellet, which was then resuspended in 1 ml of diethyl pyrocarbonate-treated water (Ambion). A volume of 10 μl of lysozyme (50 mg ml^{-1}), 5 μg of proteinase K (20 mg ml^{-1}), and 30 μl of 10% sodium dodecyl sulfate solution were added and the mixture was heated to 37 °C for 10 min. The supernatant was separated by centrifugation at $16\,000 \times g$ for 15 min. Plant RNA Isolation Aid (50 μl), 10 μl of tRNA (10 mg ml^{-1}; Ambion), 600 μl of heated acidic phenol (pH 4.5, 70 °C, Ambion), and 400 μl of chloroform: isoamyl alcohol (24:1, Sigma, St Louis, MO, USA) were added. The supernatant was mixed on a rotary shaker for 5 min and then centrifuged at $16\,000 \times g$ for 5 min. The aqueous layer was removed and mixed with 100 μl 5 N NH_4OAc (Ambion), 20 μl glycogen (Ambion) and 1 ml of −20 °C isopropanol (Sigma). The RNA was precipitated for 1 h at −20 °C, centrifuged at $16\,000 \times g$ for 30 min and washed with 70% EtOH at −20 °C. Pellets where then dried at room temperature and resuspended in 50 μl of diethyl pyrocarbonate-treated water.

Resuspended pellets were cleaned with RNeasy RNA clean up kit (Qiagen) and DNA-free DNase Kit (Ambion) following the manufactures' instructions and tested for genomic DNA contamination as previously described (Postier *et al.*, 2008).

The RNA extracts had A260/280 ratios, as determined with a Nanodrop ND-1000 spectrophotometer (NanoDrop Technologies, Wilmington, DE, USA), of 1.8–2.0, indicating high purity (Ausubel *et al.*, 1997). Total RNA (0.5 μg) was amplified and biotin-labeled using the MessageAmp II-Bacteria Kit (Ambion) as previously described (Postier *et al.*, 2008) following the manufacturer's instructions.

Synthesis of cDNA, array hybridization and imaging were performed at the Genomic Core Facility at the University of Massachusetts Medical Center. A total of 10 μg of amplified cRNA was used as template to synthesize labeled cDNAs using Affymetrix (Santa Clara, CA, USA) GeneChip DNA Labeling Reagent Kits. Labeled cDNA samples were hybridized to Affymtrix GeneChip *G. sulfurreducens* arrays according to Affymetrix guidelines. After hybridization, the arrays were scanned with a GeneChip 3000 Scanner and normalized gene expression data were analyzed by ArrayStar (DNASTAR, Madison, WI, USA) using the Robust Multichip Average algorithm. A Student *t*-test with a cutoff *P*-value of 0.05 was used to compare the mean gene expression value and differentially regulated genes were detected using a minimum twofold change from this group. Microarray data have been deposited with the NCBI Gene Expression Omnibus (http://www.ncbi.nlm.nih.gov/geo) under accession numbers GSE17591.

Quantitative real-time PCR (qRT–PCR) analysis

Gene expression patterns for select genes were further evaluated using quantitative RT–PCR. Forward and reverse primers were designed with Primer3 software (Rozen and Skaletsky, 2000) and are listed in Supplementary Table 1. Each reaction was performed in triplicate for each biological replicate for each gene tested.

Single strand cDNA was created through reverse transcription of 2 μg cRNA in a 100-μl reaction volume of TaqMan Reverse Transcription Reagents (Applied Biosystems, Foster City, CA, USA) as a template for real-time PCR. Forward and reverse primers were added at a final concentration of 200 nM to SYBR Green PCR Master Mix (Applied Biosystems) and 1 μl of 1:10 diluted template cDNA. The incorporation of SYBR Green dye into the PCR products was detected in real time on an ABI Prism 7900HT Sequence Detection System (Applied Biosystems). Normalization of non-PCR-related fluorescent signal variation was performed with a ROX (6-carboxyl-X-rhodamine) passive reference dye. The SYBR Green incorporation was used to determine the threshold cycle (C_t), which identifies the PCR cycle at which exponential production of the PCR amplicon begins. Standard curves were determined for each cDNA sample analyzed for each primer set. Expression was normalized to the house keeping gene *proC* (Holmes *et al.*, 2005). To verify amplification and correct amplicon size, aliquots from qRT–PCR were examined on an ethidium bromide stained 2% agarose gel.

Results and discussion

Evaluation of metabolic activity with redox stains

Current production and biofilm formation in the flow-through cells designed for real-time imaging were the same as previously reported (Franks *et al.*, 2009). A maximum current density of 3.5 A m^{-2} was achieved within 300 h of inoculation and this current level could be maintained indefinitely. As previously reported (Franks *et al.*, 2009), the biofilm covered the entire available graphite anode surface and formed pillar-structured biofilms greater than 50 μm thick (Figures 2a and 3a). Although a low shear and turbulence forces due to a low flow rate may have favored a more complex biofilm structure, this biofilm structure was similar to those observed in a diversity of other microbial fuel cell designs (Reguera *et al.*, 2006; Nevin *et al.*, 2009), suggesting that the flow of medium through the fuel cell did not alter typical biofilm morphology.

The addition of CTC resulted in a 15–20% decrease in current, consistent with the CTC serving as an electron acceptor for electrons derived from acetate oxidation. When the CTC was removed current production returned to the level observed before the addition of CTC.

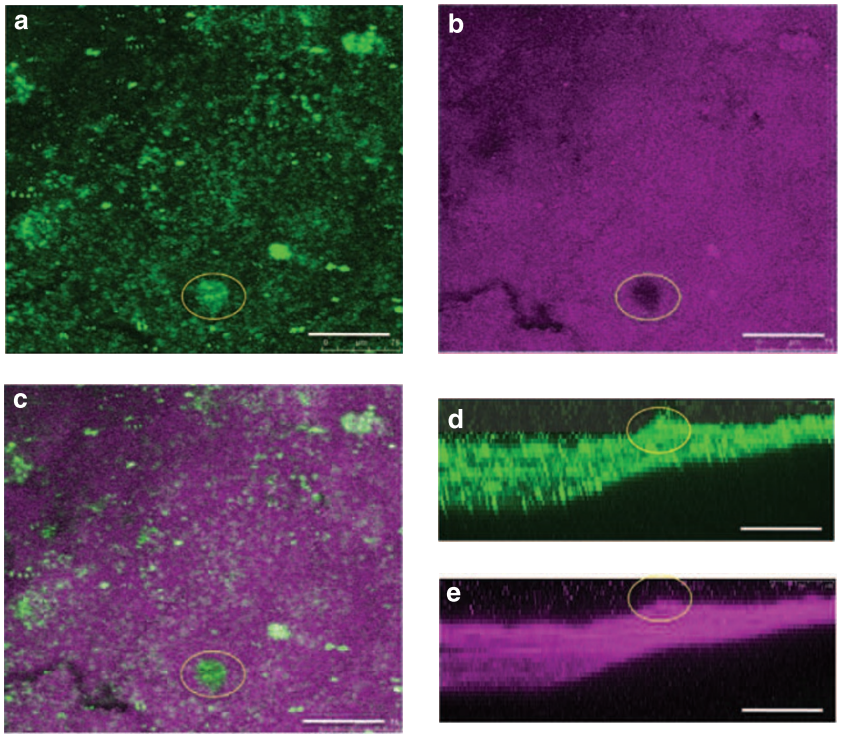

Figure 2 Confocal scanning laser micrographs of anode biofilms treated with the metabolic stain 5-cyano-2,3-ditolyl tetrazolium chloride (CTC). *Geobacter sulfurreducens* pRG5Mc, which constitutively produces the fluorescent protein mcherry, was imaged here as green. Top down three-dimensional images of the cellular biomass (**a**), the purple insoluble formazan produced from the microbial reduction of CTC (**b**) and both images superimposed (**c**). Biomass (**d**) and formazan (**e**) in perpendicular cross-sections. The circled areas illustrate rare zones within (**b** and **c**) or on the outer surface (**d** and **e**) of the biofilm in which the cells did not reduce CTC. White bar = 75 μm.

After staining the current-producing biofilm with the CTC, the red fluorescent formazan that is a product of microbial reduction of CTC could be detected, but only were cells were present (Figure 2c). The CTC level was reduced through out most of the biofilm (Figures 2b and c), including the outer pillared structures that reached up to 50 μm from the anode surface. There were a few isolated zones within the biofilms that did not reduce CTC and were apparently metabolically inactive (Figures 2b and c). In rare instances, the cells in the very top of a pillar (~50 μm from the anode surface) did not reduce CTC, indicating that, sporadically, there was a lack of metabolic activity at this outer fringe of the biofilm (Figures 2d and f). These results suggested that the vast majority of the cells within the cells had the potential for metabolic activity.

This conclusion was supported in additional studies in which the capacity for electron transfer was evaluated with Redox Green (Figure 3). The spatial pattern of Redox Green reduction was similar to that for CTC reduction (Figures 3a and b). Reductase activity was observed throughout the entire biofilm with only rare spots within the biofilm (Figure 3c), or at outer surface (Figures 3d and e), in which the metabolic stain was not reduced.

Transcriptional analysis of outer versus inner members of current-producing biofilms

To obtain more detailed information on metabolic status of cells within the biofilm, gene transcript abundance in cells growing near the anode was compared with those at the outer surface with whole-genome microarray analysis. Current production (Figure 4a) in the flow-through 'H-cell' design with the 'fingered' graphite anodes that permitted portions of the anode to be cut for microtoming was comparable to the power production previously reported for the same type of H-cells with the previously used solid graphite stick anodes (Nevin *et al*., 2009). The biofilm was comprised of a layer ca. 30-μm thick, which completely covered the entire surface with differentiated pillar structures up to 55-μm thick (Figures 4b and c).

A total 146 genes were identified as being differentially expressed ($P<0.05$) between the inner (0–20 μm) and outer (30–60 μm) portions of the biofilm using a twofold cut off in expression (Supplementary Table 2). *GSU0093*, the only gene more highly expressed (2.1-fold) in the cells in the outer portion of the biofilm compared with the inner portion, encodes a putative ATP-binding cassette transporter, ATP-binding/membrane protein. There are homologs of GSU0093 in other *Geobacter* species, including *G. metallireducens*, *G. daltonii*

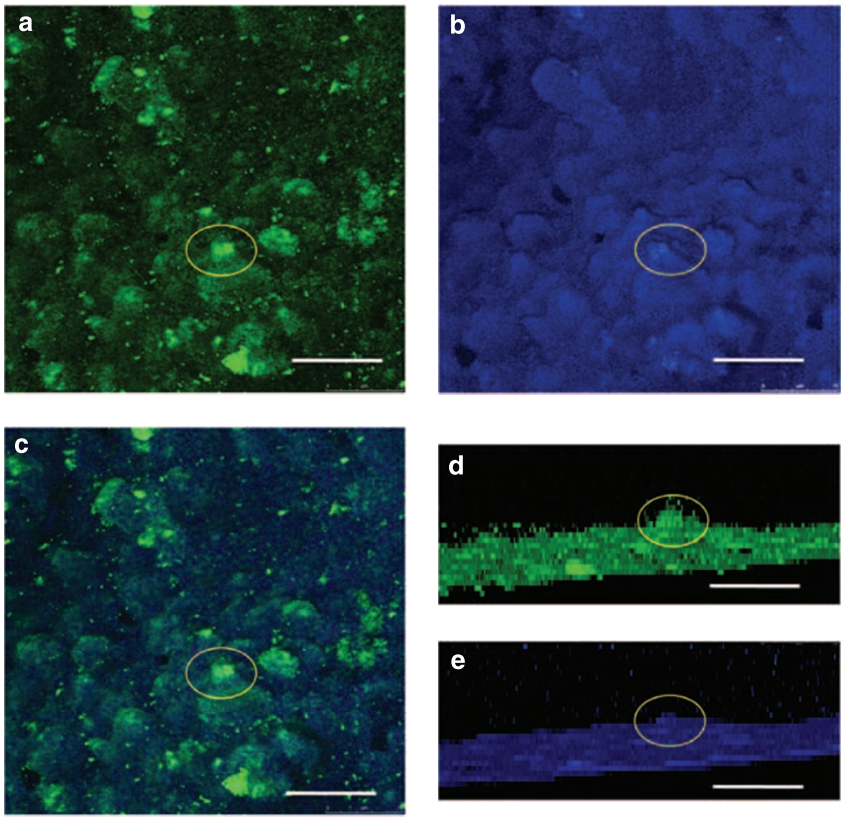

Figure 3 Confocal scanning laser micrographs of anode biofilms of *Geobacter sulfurreducens* pRG5Mc treated with Redox Green reagent. Biomass imaged in green as in Figure 1. Top down three-dimensional images of the cellular biomass (**a**), the blue reduced redox green (**b**) and both images superimposed (**c**). Biomass (**d**) and reduced redox green (**e**) in perpendicular cross-sections. The circled areas illustrate rare zones within (**b** and **c**) or on the outer surface (**d** and **e**) in which the cells did not reduce CTC. White bar = 75 μm.

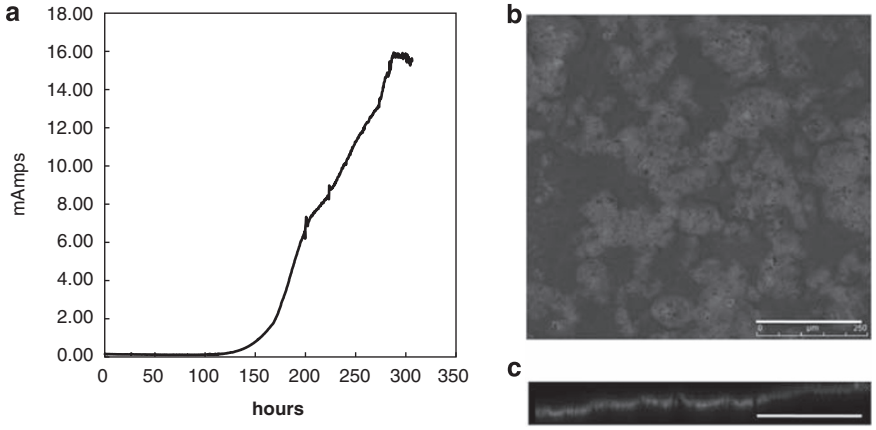

Figure 4 Power production (**a**) and confocal scanning laser micrograph of biofilm formation on graphite anodes used for microarray analysis represented as three-dimensional image (**b**) and in perpendicular cross sections (**c**). Cells were imaged with Live/Dead stain. White bar = 250 μm.

(formerly strain FRC-32), *G. uraniireducens*, *G. bemidjiensis*, *Geobacter* strain M21 and *G. lovleyi*. The function of this gene, and hence the significance of its increased expression in the outer portion of the anode biofilm, is unknown.

The transcript levels of a number of ribosomal protein-encoding genes had a ca. 2–3-fold lower abundance in cells in the outer layer of the biofilm (Supplementary Table 3). Greater ribosome production is associated with faster growth rates in many microorganisms (Wagner, 1994; Hua *et al.*, 2004; Beste *et al.*, 2005; Boccazzi *et al.*, 2005) and there was more ribosomal protein in faster growing cultures of *G. sulfurreducens* (Ding *et al.*, 2006). In the closely related *G. uraniireducnes*, transcript abundance for ribosomal protein genes was related

to growth rate (Holmes *et al.*, 2009). Thus, the slightly lower abundance of ribosomal protein gene transcripts in the outer layer of the biofilm suggests that those cells might be growing slower.

Further evidence for slightly slower metabolic rates in the cells in the outer portion of the biofilm was the finding that genes in the *nuo* operon (GSU0338–GSU0351) had lower (ca. 1.6–2.8-fold) transcript levels in the outer biofilm. Genes in the *nuo* cluster encode components of a large membrane-associated NADH dehydrogenase that transfers reducing equivalents generated in the TCA cycle to the menaquinone pool (Izallalen *et al.*, 2008).

However, differences in the rates of metabolism between the inner and outer layer are unlikely to have been substantial because there was not a significant difference in the abundance of transcripts for genes encoding proteins of the TCA cycle. For example, transcript levels for *gltA*, which encodes a subunit of citrate synthase in *G. sulfurreducens* (Bond *et al.*, 2005), is directly related to metabolic rates, including electron transfer to electrodes (Holmes *et al.*, 2005). A similar response is expected for other TCA cycle enzyme genes (Holmes *et al.*, 2008, 2009). In general, values for transcript abundance of TCA cycle genes seemed to be lower in the samples from the outer layer of the biofilm, but the differences were small (<two-fold) and not statistically significant. Quantitative RT–PCR analysis of *gltA* transcript levels indicated that the difference between the inner and outer layers was only 1.3-fold.

Transcripts for outer-surface electron-transfer components, considered important for electron transfer at the anode, were similar in the inner and outer sections of the biofilms. For example, a previous comparison between gene expression in *G. sulfurreducens* biofilms producing current versus biofilms growing on the same surface material, but using fumarate as the electron acceptor (Nevin *et al.*, 2009), revealed increased expression of the gene for PilA, the structural protein for the pili that seem to be electrically conductive pili (Reguera *et al.*, 2005) and may be involved in electron transfer through anode biofilms (Reguera *et al.*, 2006; Nevin *et al.*, 2009). Cells in the inner and outer portions of the biofilm did not have a significant difference in *pilA* expression, but the adjacent gene, *GSU1497*, was less expressed (2.6-fold) in the outer biofilm (Nevin *et al.*, 2009).

OmcZ is an outer-surface, *c*-type cytochrome that is essential for high-density current production and the *OmcZ* gene is more highly expressed in current-producing cells (Nevin *et al.*, 2009; Richter *et al.*, 2009). Expression of *omcZ* was similar in the inner and outer biofilm. Two other outer-surface *c*-type cytochromes, OmcB and OmcE, which are also more highly expressed in current-producing cells versus cells reducing fumarate (Nevin *et al.*, 2009), were also expressed at similar levels in the inner and outer biofilm sections. The lack of significant change in the expression of any of these genes between the inner and outer portions of the biofilm suggests that the cells in both portions of the biofilm are experiencing similar requirements for extracellular electron transfer.

Transcript levels in the outer biofilm of genes for several cytochromes that do not seem to have a direct role in extracellular electron transfer were slightly (ca. 2.05–2.85-fold) decreased (Supplementary Table 4). These included two putative outer-surface *c*-type cytochromes, OmcX and OmcQ, putative cytochromes encoded by GSU0593 and GSU2743, as well as the periplasmic cytochrome PpcA (Lloyd *et al.*, 2003). However, there seemed to be no significant difference in the expression levels of the vast majority of the ca. 100 *c*-type cytochrome genes (Methé *et al.*, 2003) in *G. sulfurreducens*.

If there were substantial disparities in electron-acceptor availability between the inner and outer sections of the biofilm it might be expected that this would result in some other differences in metabolism that were not reflected in changes in gene transcript abundance. For example, *G. sulfurreducens* will reduce protons to hydrogen if alternative electron acceptors are not available (Cord-Ruwisch *et al.*, 1998). Therefore, if cells at the outer surface of the biofilm were unable to transfer electrons derived from acetate metabolism to the anode, an alternative response would be to increase hydrogen production with a corresponding increase in transcription of hydrogenase genes. However, there was no difference in expression of hydrogenase genes between the inner and outer sections of the biofilm, suggesting that the cells in the outer section did not have an electron acceptor limitation.

A potential limitation on the metabolism for cells closer to the anode surface is lack of electron donor or nutrients due to cells in the outer section consuming these components (He *et al.*, 2005; Marcus *et al.*, 2007; Rabaey *et al.*, 2007; Torres *et al.*, 2008). *G. sulfurreducens* genes encoding acetate transporters that are more highly expressed when acetate is limiting have been identified (Risso *et al.*, 2008). However, transcript abundance for these genes was comparable in the inner and outer sections of the biofilms, suggesting that acetate limitation is not an important consideration in current production. In a similar manner, genes that are more highly expressed under nitrogen- (Holmes *et al.*, 2004; Methé *et al.*, 2005; Mouser *et al.*, 2009b), iron- (O'Neil *et al.*, 2008) or phosphate-limiting (N'Guessan *et al.*, 2009) conditions had similar transcript abundances in the outer and inner portions of the biofilm.

Cells in the outer section of the biofilm had lower expression of a number of genes expression of which is expected to increase in response to environmental stress (Supplementary Table 5). These included genes encoding putative cold shock proteins, *sodA*, mscL and universal stress response proteins. The

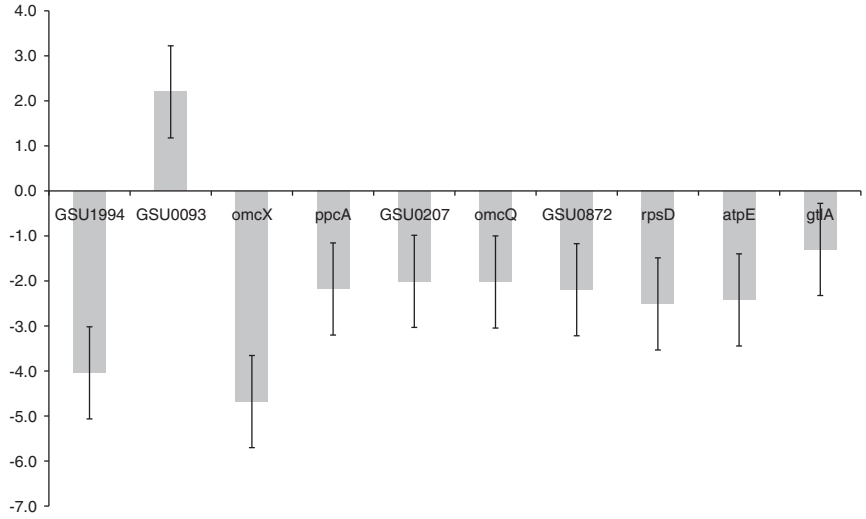

Figure 5 Fold change in transcript abundance of a diversity of genes between inner and outer biofilms as determined with quantitative RT–PCR. Error bars illustrated the s.d. values of the triplicate determinations.

greatest increase in abundance in transcripts of stress-reponse genes was for *sodA.* Although this gene is known to be involved in the oxidative stress response in some microorganisms, its role in *Geobacter* species seems to be different (Mouser *et al.*, 2009a), with highest expression associated with the use of Fe(III) as an electron acceptor (Methé *et al.*, 2005; Mouser *et al.*, 2009b). Increased expression of *mscL* in *Escherichia coli* is associated with entry into stationary phase or hyperosmotic shock (Booth *et al.*, 2007; Kloda *et al.*, 2008). Under acidic stress the regulation of numerous genes, which overlap with oxidative stress, heat shock and envelop stress responses have been identified (Maurer *et al.*, 2005). The increase in transcript abundance of these stress response genes in cells closer to the anode may be in response to the lower pH that is expected closer to the anode surface (Franks *et al.*, 2009).

As a check on the microarray results, transcript abundance was also evaluated with quantitative RT–PCR for a few select genes (Figure 5). These included: the only upregulated gene, *GSU093*; the most highly downregulated gene *GSU1994* and genes for several other hypothetical proteins; genes encoding representative ribosomal, electron transfer and energy conservation proteins; and, as noted above, the citrate synthase gene, *gtlA.* Results from the quantitative RT–PCR were comparable to the microarray results.

Implications

The results of the staining for metabolic activity, as well as the analysis of differential gene expression between the inner and outer sections of the anode biofilm suggest that cells throughout the biofilm are metabolically active and likely to be contributing to current production. Evidence for slightly lower rates of growth and metabolism in cells in the outer section of the biofilm includes transcript level differences for some ribosomal proteins and a NADH dehydrogenase. However, transcript abundances for key metabolic genes, such as citrate synthase, which previous studies have shown have significantly changes in expression levels when metabolic rates change, were not significantly different between the inner and outer fractions of the biofilm.

There also was little indication from the gene expression results that cells throughout the anode biofilms were electron donor or nutrient-limited or had significant differences in the expression of proteins thought to be important in electron transfer to the anode. Increased transcript abundance for several genes associated with stress responses in cells within the inner section of the biofilm do suggest that these cells may be under some environmental stress, possibly associated with the expected lower pH in that environment, but this apparent stress does not seem to significantly impact on metabolism.

The finding that cells throughout the bulk of the biofilm are metabolically active and likely to be contributing to current production is consistent with the previous finding of a linear increase in current production with increasing anode biomass and biofilm height (Reguera *et al.*, 2006). This requires that cells not in direct contact with the anode can still transfer electrons to the anode and it was suggested that electrically conductive pili may mediate this long-range electron transfer (Reguera *et al.*, 2006). Modeling studies have predicted that the conductivity of the biofilm would have to be 10^{-4} mS cm^{-1} to avoid electron transfer limitation (Marcus *et al.*, 2007). Although biofilms are generally considered to act as insulators rather than conductors (Herbert-Guillou *et al.*, 1999; Muñoz-Berbel *et al.*, 2006; Dheilly *et al.*, 2008), the finding that cells at substantial distance from the anode are

metabolically active is consisent with the concept that anode biofilms may be conductive.

Clearly, the more cells that can release electrons from metabolic activity, the greater the potential current output. However, there do seem to be limits on how thick anode biofilms can grow and metabolic staining provided evidence that some cells in the most outer surface of the biofilm may not metabolically active. The factors limiting metabolism in the small areas at the outer reaches of the biofilm are yet not understood, but overcoming these limitations could be a useful strategy for increasing the power output of microbial fuel cells.

The microtoming–microarray approach for depth resolution of gene expression in biofilms described here may be applicable to the study of gene expression in other types of biofilms. Genes specifically expressed during biofilm formation in response to environmental conditions or specific mutations have been identified (Whiteley *et al.*, 2001; Schembri *et al.*, 2003; Stanley *et al.*, 2003; Zhu and Mekalanos, 2003), but these studies on whole biofilms lacked the spatial resolution that may be necessary to account for the heterogeneity in metabolic states that can be expected in biofilms (Stewart and Franklin, 2008). Introducing reporters that express unstable green fluorescent proteins can provide insight into the expression of individual genes throughout biofilms (Sternberg *et al.*, 1999; Teal *et al.*, 2006; Stewart and Franklin, 2008). However, this strategy is limited to evaluating the expression of a small number of genes and cannot be applied to microorganisms for which systems for genetic manipulation have not been developed. The microtoming–microarray approach described here can be applied to any organism for which a genome sequence is available. Furthermore, it could readily be adapted for the study of multi-species biofilms or natural biofilm communities with the appropriate metagenomic/metatranscriptomic approaches.

Acknowledgements

We thank L Raboin, Polymer Science, University of Massachusetts, Amherst, for his help and suggestions with the microtoming procedure and Dr H Bagdadi for discussions leading to the development of this approach. This study was supported by the Office of Science (BER), U.S. Department of Energy, Cooperative Agreement No. DE-FC02–02ER63446 and Office of Naval Research Award No. N00014-07-1-0966.

References

An D, Parsek MR. (2007). The promise and peril of transcriptional profiling in biofilm communities. *Curr Opin Microbiol* **10**: 292–296.

Ausubel FM, Brent R, Kingston RE, Moore DD, Seidman JG, Smith JA *et al.* (1997). *Current Protocols in Molecular Biology*. John Wiley and Sons, Inc.: New York.

Beste DJV, Peters J, Hooper T, Avignone-Rossa C, Bushell ME, McFadden J. (2005). Compiling a molecular inventory for *Mycobacterium bovis* BCG at two growth rates: evidence for growth rate-mediated regulation of ribosome biosynthesis and lipid metabolism. *J Bacteriol* **187**: 1677–1684.

Bhupathiraju VK, Hernandez M, Landfear D, Alvarez-Cohen L. (1999). Application of a tetrazolium dye as an indicator of viability in anaerobic bacteria. *J Microbiol Methods* **37**: 231–243.

Boccazzi P, Zanzotto A, Szita A, Bhattacharya S, Jensen KF, Sinskey AJ. (2005). Gene expression analysis of *Escherichia coli* grown in miniaturized bioreactor platforms for high-throughput analysis of growth and genomic data. *App Microbiol Biotechnol* **68**: 518–532.

Bond DR, Mester T, Nesbø CL, Izquierdo-Lopez AV, Collart FL, Lovley DR. (2005). Characterization of citrate synthase from *Geobacter sulfurreducens* and evidence for a family of citrate synthases similar to those of eukaryotes throughout the *Geobacteraceae*. *Appl Environ Microbiol* **71**: 3858–3865.

Booth IR, Edwards MD, Black S, Schumann U, Miller S. (2007). Mechanosensitive channels in bacteria: signs of closure? *Nat Rev Microbiol* **5**: 431–440.

Boulos L, Prévost M, Barbeau B, Coallier J, Desjardins R. (1999). LIVE/DEAD BacLight: application of a new rapid staining method for direct enumeration of viable and total bacteria in drinking water. *J Microbiol Methods* **37**: 77–86.

Caccavo F, Lonergan DJ, Lovely DR, Davis M, Stolz JF, Mcinerney MJ. (1994). *Geobacter sulfurreducens* sp. nov., a hydrogen- and acetate-oxidizing dissimilatory metal-reducing microorganism. *Appl Environ Microbiol* **60**: 3752–3759.

Cord-Ruwisch R, Lovley DR, Schink B. (1998). Growth of *Geobacter sulfurreducens* with acetate in syntrophic cooperation with hydrogen-oxidizing anaerobic partners. *Appl Environ Microbiol* **64**: 2232–2236.

Dheilly A, Linossier I, Darchen A, Hadjiev D, Corbel C, Alonso V. (2008). Monitoring of microbial adhesion and biofilm growth using electrochemical impedancemetry. *Appl Microbiol Biotechnol* **79**: 157–164.

Ding YH, Hixson KK, Giometti CS, Stanley A, Esteve-Núñez A, Khare T *et al.* (2006). The proteome of dissimilatory metal-reducing microorganism *Geobacter sulfurreducens* under various growth conditions. *Biochim Biophys Acta* **1764**: 1198–1206.

Franks AE, Nevin KP, Jia H, Izallalen M, Woodard TL, Lovley DR. (2009). Novel strategy for three-dimensional real-time imaging of microbial fuel cell communities: monitoring the inhibitory effects of proton accumulation within the anode biofilm. *Energy Enviro Sci* **2**: 113–119.

Gray D, Yue RS, Chueng CY, Godfrey W. (2005). Bacterial vitality detected by a novel fluorogenic redox dye using flow cytometry. In: Abstracts of the American Society of Microbiology Meeting American Society for Microbiology: Washington, DC, USA.

Gruden CL, Fevig S, Abu-Dalo M, Hernandez M. (2003). 5-Cyano-2,3-ditolyl tetrazolium chloride (CTC) reduction in a mesophilic anaerobic digester: Measuring redox behavior, differentiating abiotic reduction, and comparing FISH response as an activity indicator. *J Microbiol Methods* **52**: 59–68.

He Z, Minteer SD, Angenent LT. (2005). Electricity generation from artificial wastewater using an

upflow microbial fuel cell. *Environ Sci Technol* **39**: 5262–5267.

Herbert-Guillou D, Tribollet B, Festy D, Kiéné L. (1999). *In situ* detection and characterization of biofilm in waters by electrochemical methods. *Electrochimica Acta* **45**: 1067–1075.

Holmes DE, Mester T, O'Neil RA, Perpetua LA, Larrahondo MJ, Glaven R *et al.* (2008). Genes for two multicopper proteins required for Fe(III) oxide reduction in *Geobacter sulfurreducens* have different expression patterns both in the subsurface and on energy-harvesting electrodes. *Microbiol* **154**: 1422–1435.

Holmes DE, Nevin KP, Lovley DR. (2004). *In situ* expression of *Geobacteraceae nifD* in subsurface sediments. *Appl Environ Microbiol* **70**: 7251–7259.

Holmes DE, Nevin KP, O'Neil RA, Ward JE, Adams LA, Woodard TL *et al.* (2005). Potential for quantifying expression of the *Geobacteraceae* citrate synthase gene to assess the activity of *Geobacteraceae* in the subsurface and on current-harvesting electrodes. *Appl Environ Microbiol* **71**: 6870–6877.

Holmes DE, O'Neil RA, Chavan MA, N'Guessan LA, Vrionis HA, Perpetua LA *et al.* (2009). Transcriptome of *Geobacter uraniireducens* growing in uranium-contaminated subsurface sediments. *ISME J* **3**: 216–230.

Hua Q, Yang C, Oshima T, Mori H, Shimizu K. (2004). Analysis of gene expression in escherichia coli in response to changes of growth-limiting nutrient in chemostat cultures. *Appl Environ Microbiol* **70**: 2354–2366.

Huang CT, Yu FP, McFeters GA, Stewart PS. (1995). Nonuniform spatial patterns of respiratory activity within biofilms during disinfection. *Appl Environ Microbiol* **61**: 2252–2256.

Izallalen M, Mahadevan R, Burgard A, Postier B, Didonato Jr R, Sun J *et al.* (2008). *Geobacter sulfurreducens* strain engineered for increased rates of respiration. *Metab Eng* **10**: 267–275.

Kalyuzhnaya MG, Lidstrom ME, Chistoserdova L. (2008). Real-time detection of actively metabolizing microbes by redox sensing as applied to methylotroph populations in Lake Washington. *ISME J* **2**: 696–706.

Kloda A, Petrov E, Meyer GR, Nguyen T, Hurst AC, Hool L *et al.* (2008). Mechanosensitive channel of large conductance. *Int J Biochem Cell Biol* **40**: 164–169.

Lloyd JR, Leang C, Hodges Myerson AL, Coppi MV, Cuifo S, Methe B *et al.* (2003). Biochemical and genetic characterization of PpcA, a periplasmic *c*-type cytochrome in *Geobacter sulfurreducens*. *Biochem J* **369**: 153–161.

Logan BE. (2009). Exoelectrogenic bacteria that power microbial fuel cells. *Nat Rev Microbiol* **7**: 375–381.

Logan BE, Regan JM. (2006). Electricity-producing bacterial communities in microbial fuel cells. *Trends Microbiol* **14**: 512–518.

Lovley DR. (2006). Bug juice: harvesting electricity with microorganisms. *Nat Rev Microbiol* **4**: 497–508.

Lovley DR. (2008). The microbe electric: conversion of organic matter to electricity. *Curr Opin Biotechnol* **19**: 564–571.

Marcus AK, Torres CI, Rittmann BE. (2007). Conduction-based modeling of the biofilm anode of a microbial fuel cell. *Biotechnol Bioeng* **98**: 1171–1182.

Maurer LM, Yohannes E, Bondurant SS, Radmacher M, Slonczewski JL. (2005). pH regulates genes for flagellar motility, catabolism, and oxidative stress in *Escherichia coli* K-12. *J Bacteriol* **187**: 304–319.

Methé BA, Nelson KE, Eisen JA, Paulsen IT, Nelson W, Heidelberg JF *et al.* (2003). The genome of *Geobacter sulfurreducens*: insights into metal reduction in subsurface environments. *Science* **302**: 1967–1969.

Methé BA, Webster J, Nevin K, Butler J, Lovley DR. (2005). DNA microarray analysis of nitrogen fixation and Fe(III) reduction in *Geobacter sulfurreducens*. *Appl Environ Microbiol* **71**: 2530–2538.

Mouser PJ, Holmes DE, Perpetua LA, DiDonato R, Postier B, Liu A *et al.* (2009a). Quantifying expression of *Geobacter* spp. oxidative stress genes in pure culture and during *in situ* uranium bioremediation. *ISME J* **3**: 454–465.

Mouser PJ, N'Guessan AL, Elifantz H, Holmes DE, Williams KH, Wilkins MJ *et al.* (2009b). Influence of heterogeneous ammonium availability on bacterial community structure and the expression of nitrogen fixation and ammonium transporter genes during *in situ* bioremediation of uranium-contaminated groundwater. *Environ Sci Technol* **43**: 4386–4392.

Muñoz-Berbel X, Muñoz FJ, Vigués N, Mas J. (2006). On-chip impedance measurements to monitor biofilm formation in the drinking water distribution network. *Sens Actuators: B Chem* **118**: 129–134.

Nevin KP, Kim BC, Glaven RH, Johnson JP, Woodard TL, Methé BA *et al.* (2009). Anode biofilm transcriptomics reveals outer surface components essential for high density current production in *Geobacter sulfurreducens* fuel cells. *PLoS ONE* **4**: e5628.

N'Guessan AL, Elifantz H, Nevin KP, Mouser PJ *et al.* (2009). Molecular analysis of phosphate limitation in *Geobacteraceae* during the bioremediation of a uranium-contaminated aquifer. *ISME J* (in press).

O'Neil RA, Holmes DE, Coppi MV, Adams LA, Larrahondo MJ, Ward JE *et al.* (2008). Gene transcript analysis of assimilatory iron limitation in *Geobacteraceae* during groundwater bioremediation. *Environ Microbiol* **10**: 1218–1230.

Postier B, DiDonato R, Nevin KP, Liu A, Frank B, Lovley DR *et al.* (2008). Benefits of electrochemically synthesized oligonucleotide microarrays for analysis of gene expression in understudied microorganisms. *J Microbiol Methods* **74**: 26–32.

Rabaey K, Rodríguez J, Blackall LL, Keller J, Gross P, Batstone D *et al.* (2007). Microbial ecology meets electrochemistry: electricity-driven and driving communities. *ISME J* **1**: 9–18.

Reguera G, McCarthy KD, Mehta T, Nicoll JS, Tuominen MT, Lovely DR. (2005). Extracellular electron transfer via microbial nanowires. *Nature* **435**: 1098–1101.

Reguera G, Nevin KP, Nicoll JS, Covalla SF, Woodard TL, Lovley DR *et al.* (2006). Biofilm and nanowire production leads to increased current in *Geobacter sulfurreducens* fuel cells. *Appl Environ Microbiol* **72**: 7345–7348.

Richter H, Nevin KP, Jia H, Lowy DA, Lovley DR, Tender LM. (2009). Cyclic voltammetry of biofilms of wild type and mutant *Geobacter sulfurreducens* on fuel cell anodes indicates possible roles of OmcB, OmcZ, type IV pili, and protons in extracellular electron transfer. *Energy Environ Sci* **2**: 506–516.

Risso C, Methé BA, Elifantz H, Holmes DE, Lovley DR. (2008). Highly conserved genes in *Geobacter* species

with expression patterns indicative of acetate limitation. *Microbiol* **154**: 2589–2599.

Rittmann BE, Torres CI, Marcus AK. (2008). Understanding the distinguishing features of a microbial fuel cell as a biomass-based renewable energy technology. In: Shah V (ed). *Emerging Environmental Technologies*. Springer Netherlands: Netherlands, pp 1–28.

Rodriguez GG, Phipps D, Ishiguro K, Ridgway HF. (1992). Use of a fluorescent redox probe for direct visualization of actively respiring bacteria. *Appl Environ Microbiol* **58**: 1801–1808.

Rozen S, Skaletsky H. (2000). Primer3 on the WWW for general users and for biologist programmers. In: Krawetz S, Misener S (eds). *Bioinformatics Methods and Protocols: Methods in Molecular Biology*. Humana Press: Totowa, NJ, 365–386.

Schaule G, Flemming HC, Ridgway HF. (1993). Use of 5-cyano-2,3-ditolyl tetrazolium chloride for quantifying planktonic and sessile respiring bacteria in drinking water. *Appl Environ Microbiol* **59**: 3850–3857.

Schembri MA, Kjaergaard K, Klemm P. (2003). Global gene expression in *Escherichia coli* biofilms. *Mol Microbiol* **48**: 253–267.

Stanley NR, Britton RA, Grossman AD, Lazazzera BA. (2003). Identification of catabolite repression as a physiological regulator of biofilm formation by *Bacillus subtilis* by use of DNA microarrays. *J Bacteriol* **185**: 1951–1957.

Stewart PS, Franklin MJ. (2008). Physiological heterogeneity in biofilms. *Nat Rev Microbiol* **6**: 199–210.

Sternberg C, Christensen BB, Johansen T, Toftgaard Nielsen A, Andersen JB, Givskov M *et al.* (1999). Distribution of bacterial growth activity in flow-chamber biofilms. *Appl Environ Microbiol* **65**: 4108–4117.

Teal TK, Lies DP, Wold BJ, Newman DK. (2006). Spatiometabolic stratification of *Shewanella oneidensis* biofilms. *Appl Environ Microbiol* **72**: 7324–7330.

Torres CI, Marcus AK, Rittmann BE. (2008). Proton transport inside the biofilm limits electrical current generation by anode-respiring bacteria. *Biotechnol Bioeng* **100**: 872–881.

Wagner R. (1994). The regulation of ribosomal RNA synthesis and bacterial cell growth. *Arch Microbiol* **161**: 100–109.

Whiteley M, Bangera MG, Bumgarner RE, Parsek MR, Teitzel GM, Lory S *et al.* (2001). Gene expression in *Pseudomonas aeruginosa* biofilms. *Nature* **413**: 860–864.

Zheng Z, Stewart PS. (2004). Growth limitation of *Staphylococcus epidermidis* in biofilms contributes to rifampin tolerance. *Biofilms* **1**: 31–35.

Zhu J, Mekalanos JJ. (2003). Quorum sensing-dependent biofilms enhance colonization in *Vibrio cholerae*. *Dev Cell* **5**: 647–656.

Supplementary Information accompanies the paper on The ISME Journal website (http://www.nature.com/ismej)